Magnetostatic Wave Propagation in a Finite YIG-Loaded Rectangular Waveguide

MASSOUDE RADMANESH, CHIAO-MIN CHU, AND GEORGE I. HADDAD, FELLOW, IEEE

***Abstract*—The propagation of magnetostatic waves (MSW) in a waveguide partially loaded with a low-loss ferrite slab is investigated theoretically. The most common low-loss ferrite material used for MSW propagation is epitaxial yttrium iron garnet (YIG). A YIG slab is placed inside and along the guide and not in contact with the sidewalls of the waveguide. The dc magnetic field is assumed to be parallel to the YIG slab and perpendicular to the direction of propagation. Using the integral equation method, the dispersion relation is found to be an infinitely large determinant equal to zero. Proper truncation of this determinant and numerical analysis to find its roots are carried out in this work. It is seen that in order to obtain high values of group time delay, the YIG slab must be narrow and placed at the bottom of the guide. On the other hand, to maximize the device bandwidth, a narrow YIG slab positioned at the top inside surface of the waveguide is preferred. It is also noticed that there exists a tradeoff between the time delay and the device bandwidth and that maximization of one property leads to a poor value in the other. Thus, some design compromises should be made. It is also observed that the frequency range of operation of the device can be adjusted by an external magnetic bias field. This property of tuning the device to operate in any frequency range adds an extra dimension of flexibility to the operation and also to the design of these devices.**

I. Introduction

MAGNETOSTATIC-WAVE PROPAGATION in a yttrium iron garnet (YIG) slab in free space on an infinite ground plane or bounded by two infinite parallel ground planes or completely filling a waveguide has been reported in previous papers [1]–[3]. Some results pertinent to the design and construction of delay lines and filters were also given [4]–[6]. The theoretical analysis carried out by all these earlier works is based on the method of separation of variables, whereby a closed form for the dispersion relation may be obtained. The case of magnetostatic-wave (MSW) propagation in a YIG slab enclosed in a waveguide as illustrated in Fig. 1 has never been studied. In this paper, the propagation of magnetostatic waves in a rectangular waveguide partially filled with a YIG slab is studied theoretically. The dc external magnetic field is parallel to the slab and perpendicular to the direction of propagation. The slab is placed inside and along the guide but not necessarily in contact with the waveguide walls. To simplify the analysis, the slab is assumed to be thin, so that approximate numerical solution becomes feasible.

Manuscript received March 13, 1986; revised June 20, 1986. This work was supported in part by the Air Force Systems Command, Avionics Laboratory, Wright-Patterson Air Force Base, OH, under Contract F33615-81-8-1429.

M. Radmanesh is with the GMI Engineering and Management Institute, Electrical and Computer Engineering Department, Flint, MI 48502-2276.

C. M. Chu and G. I. Haddad are with the Department of Electrical and Computer Engineering, University of Michigan, Ann Arbor, MI 48109.

IEEE Log Number 8610565.

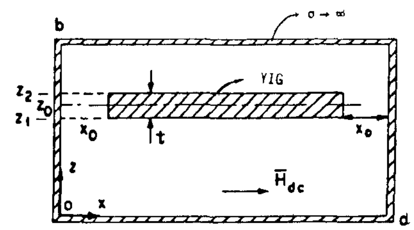

Fig. 1. Device configuration.

The introduction of a gap length (x_0) is motivated to account for the loose contacts between the YIG slab and waveguide walls and to provide a general structure for the design of delay lines.

For the configuration shown in Fig. 1, if the gap length (x_0) is zero, conventional mode analysis may be used to solve for the dispersion relation [7]. However, when x_0 is nonzero, numerical analysis based on the integral equation formulation appears to be the only means.

Based on the integral equation method, the problem of magnetostatic-wave propagation in a YIG slab of finite width inside a waveguide (Fig. 1) is analyzed, and the magnetic potential function in terms of an integral equation is derived in Section II. In Section III, an approximate numerical solution to the integral equation worked out in the earlier section is developed. Computer results based on the approximate solution for the dispersion relation and group time delay per unit length in a certain frequency range are presented in Section IV. A brief conclusion and some final discussions follow in Section V.

II. The Integral Equation Method

As noted earlier, when the width of the slab is less than the width of the waveguide, that is, when $x_0 \neq 0$ (Fig. 1), the mode analysis method appears to be fruitless and the integral equation method seems to be more appropriate. The analysis developed in this section is based on this latter method. In this method, an integral equation for the magnetic potential function inside the YIG region is deduced in steps as described below. The implied time dependence (t) is assumed to be of the form $e^{j\omega t}$ (where ω is the angular frequency) and for simplicity is omitted in all of the following expressions.

1) Assuming wave propagation in the y-direction, the y-variation of all functions involved in this study is there-

fore of the form e^{-jKy}, where K is the wavenumber. In this manner, the magnetic potential function $\psi(x, y, z)$ inside the YIG region can be written as

$$\psi(x, y, z) = \phi(x, z) e^{-jKy}. \quad (1)$$

Then, except for the common factor e^{-jKy}, the small-signal magnetic field intensity $\bar{h}$, the small-signal magnetic flux density $\bar{b}$, and the small-signal magnetization $\bar{m}$ in the YIG region are given as follows:

$$\bar{h} = \nabla\phi - jK\phi\hat{y} \quad (2)$$

$$\bar{b} = \mu_0 \bar{\bar{\mu}}_r \cdot \bar{h} \quad (3)$$

$$\bar{m} = \left(\bar{\bar{\mu}}_r - \bar{\bar{I}}\right) \cdot \bar{h} \quad (4)$$

where $\bar{\bar{I}}$ is the identity tensor and $\bar{\bar{\mu}}_r$ is the relative permeability tensor defined as

$$\bar{\bar{I}} = \begin{pmatrix} 1 & 0 & 0 \\ 0 & 1 & 0 \\ 0 & 0 & 1 \end{pmatrix} \quad (5)$$

$$\bar{\bar{\mu}}_r = \begin{pmatrix} 1 & 0 & 0 \\ 0 & \mu & jK_1 \\ 0 & -jK_1 & \mu \end{pmatrix} \quad (6)$$

and

$$\mu = 1 + \omega_0 \omega_M / \left(\omega_0^2 - \omega^2\right)$$

$$K_1 = \omega \omega_M / \left(\omega_0^2 - \omega^2\right)$$

$$\omega_0 = \mu_0 \gamma H_0, \qquad \omega_M = \mu_0 \gamma M_0.$$

μ_0 and γ are the free-space permeability constant and gyromagnetic ratio (= 2.8 MHz/Oe), respectively, ω is the operating frequency in radians, and H_0 and M_0 are the internal magnetic field and saturation magnetization, respectively [8].

Note that the internal magnetic field (H_0) is given by $H_0 = H_{dc} - N_x M_0$, where N_x is the demagnetizing factor in the x-direction. For a thin slab with the z-axis perpendicular to the broad face, $N_x = 0$ [9]. Therefore, in this analysis to the first order of approximation, the demagnetizing fields are assumed to be negligible and $H_0 = H_{dc}$.

2) From $\bar{m}$ above, the magnetic sources can be obtained. The total magnetic charge density consists of two parts: a) the magnetic volume charge density (ρ_v) and b) the magnetic surface charge density (ρ_s). These magnetic sources can be expressed as

$$\rho_v = -\nabla \cdot \bar{m} + jKm_y \quad (7)$$

$$\rho_s = \bar{m} \cdot \hat{n} \quad (8)$$

where $\hat{n}$ is a unit vector normal to the slab surface. Substituting (4) in (7) and (8) yields

$$\rho_v(x, z) = K^2(\mu - 1)\phi(x, z) - (\mu - 1)\left(\partial^2\phi(x, z)/\partial^2 z\right) \quad (9)$$

and

$$\rho_s(x, z) = \begin{cases} K_1 K\phi(x, z_1) - (\mu - 1)\,\partial\phi(x, z_1)/\partial z, & z = z_1 \quad (10a) \\ -K_1 K\phi(x, z_2) + (\mu - 1)\,\partial\phi(x, z_2)/\partial z, & z = z_2. \quad (10b) \end{cases}$$

It is to be noted that there are no surface charges at surfaces $x = x_0$ or $x = a - x_0$.

3) The Green's function, $G(x, z)e^{-jKy}$, for a magnetic line source located at (x', z') inside a waveguide satisfies

$$\left(\partial^2/\partial x^2 + \partial^2/\partial z^2\right) G(x, z) - K^2 G(x, z) = \delta(x - x')\delta(z - z'). \quad (11)$$

The solution to (11) which satisfies the following boundary conditions

$$(\partial G/\partial x) = 0, \qquad \text{at } x = 0, a$$

$$(\partial G/\partial z) = 0, \qquad \text{at } z = 0, b$$

is given by

$$G(x, x', z, z') = \sum_{n=0}^{\infty} A_n \cos n\pi x'/a \cdot \cos n\pi x/a \cosh \gamma_n'(b - z') \cosh \gamma_n' z \quad (12a)$$

for $z < z'$, and by

$$G(x, x', z, z') = \sum_{n=0}^{\infty} A_n \cos n\pi x'/a \cdot \cos n\pi x/a \cosh \gamma_n' z' \cosh \gamma_n'(b - z) \quad (12b)$$

for $z > z'$, where

$$A_n = \frac{-2}{\gamma_n' a (1 + \delta_{on}) \sinh \gamma_n' b}$$

$$\gamma_n' = \left[K^2 + (n\pi/a)^2\right]^{1/2}$$

and

$$\delta_{on} = \begin{cases} 1, & n = 0 \\ 0, & n \neq 0. \end{cases}$$

4) Considering a uniform guide cross section, the magnetic potential function can be written as

$$\phi(x, z) = \iint_{\substack{\text{YIG}\\ \text{area}}} \rho_v(x', z') G(x, x', z, z')\, dx'\, dz' + \int_{\substack{\text{YIG}\\ \text{sides}}} \rho_s(x', z') G(x, x', z, z')\, dx'. \quad (13)$$

Using (9), (10), (12), and (13), we obtain the following integral equation for $\phi(x, z)$ in the YIG region (i.e., $z_1 \leqslant z \leqslant z_2$, $x_0 \leqslant x \leqslant a - x_0$):

$$\begin{aligned} \phi(x, z) = \int_{x_0}^{a - x_0} \int_{z_1}^{z_2} & \left[K^2(\mu - 1)\phi(x', z') - (\mu - 1)\phi_{zz}(x', z')\right] \\ & \cdot G(x, x', z, z')\, dx'\, dz' + \int_{x_0}^{a - x_0} \left[K_1 K\phi(x', z_1) - (\mu - 1)\phi_z(x', z_1)\right] \\ & \cdot G(x, x', z, z_1)\, dx' + \int_{x_0}^{a - x_0} \left[-K_1 K\phi(x', z_2) + (\mu - 1)\phi_z(x', z_2)\right] \\ & \cdot G(x, x', z, z_2)\, dx'. \end{aligned} \quad (14)$$

III. The Approximate Numerical Solution

The two-dimensional integral equation given by (14) is difficult to solve numerically. For our problem, because the slab is assumed to be thin, $\phi(x, z)$ may be assumed to vary linearly in z.[1] Therefore, if we denote

$$\phi(x, z_1) = f_1(x) \tag{15a}$$

and

$$\phi(x, z_2) = f_2(x) \tag{15b}$$

then $\phi(x, z)$ is approximately given by

$$\phi(x, z) \simeq [f_2(x)(z - z_1) + f_1(x)(z_2 - z)]/(z_2 - z_1). \tag{16}$$

With this approximation, then

$$\partial\phi/\partial z \simeq [f_2(x) - f_1(x)]/(z_2 - z_1) \tag{17}$$

and

$$[\partial^2\phi/\partial z^2] = 0. \tag{18}$$

Introducing these approximations in (14), carrying out the integral in z, and letting $z = z_1$ and $z = z_2$, the following system of coupled equations results:

$$f_1(x) = -\sum_{n=0}^{\infty} B_n \cos n\pi x/a \,(g_{11}^n c_1^n + g_{12}^n c_2^n) \tag{19}$$

and

$$f_2(x) = -\sum_{n=0}^{\infty} B_n \cos n\pi x/a \,(g_{21}^n c_1^n + g_{22}^n c_2^n) \tag{20}$$

where

$$c_1^n = \int_{x_0}^{a - x_0} f_1(x) \cos n\pi x/a \, dx \tag{21}$$

$$c_2^n = \int_{x_0}^{a - x_0} f_2(x) \cos n\pi x/a \, dx \tag{22}$$

$$B_n = 2/[a(1 + \delta_{on})]$$

and g_{11}^n, g_{12}^n, g_{21}^n, and g_{22}^n are known constants which depend on the device geometry, wavenumber K, and parameter n.

Multiplication of (19) and (20) by $\cos m\pi x/a$ and integration along the interface from $x = x_0$ to $x = a - x_0$, yields the following infinite system of linear equations:

$$c_1^m + \sum_{n=0}^{\infty} \alpha_{mn}(g_{11}^n c_1^n + g_{12}^n c_2^n) = 0 \tag{23a}$$

$$c_2^m + \sum_{n=0}^{\infty} \alpha_{mn}(g_{21}^n c_1^n + g_{22}^n c_2^n) = 0 \tag{23b}$$

[1]Approximately, since the potential distribution in x can be expressed as summations of $\cos n\pi x/a$ and $\sin n\pi x/a$ then the potential distribution in z inside the slab must be the summations of $\cosh \gamma_n z$ and $\sinh \gamma_n z$, where γ_n is the transverse propagation constant [7] given by

$$\gamma_n = \left[K^2 + \frac{1}{\mu}(n\pi/a)^2\right]^{1/2}$$

Thus, for the first dominating mode, the thin-slab criterion for the principal dominating mode ($n = 1$) states that the slab thickness (t) should satisfy the following condition in order for the potential distribution to vary linearly in z:

$$t \ll 1/\gamma_1 \qquad (n = 1).$$

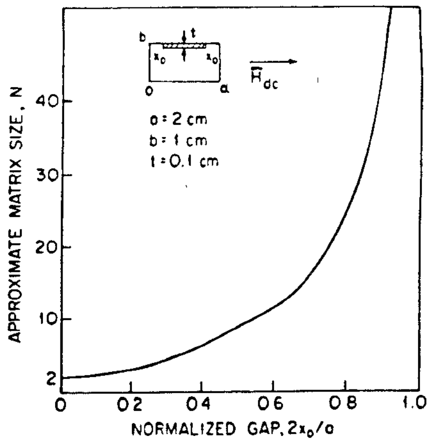

Fig. 2. Relationship of the wall gap (x_o) and the cutoff point (N).

where

$$\alpha_{mn} = \int_{x_0}^{a - x_0} B_n \cos m\pi x/a \cos n\pi x/a \, dx \qquad (m \neq 0, \quad n \neq 0). \tag{24}$$

From (23a) and (23b), it is evident that they can be decoupled into two subsystems, one for even modes and another for odd modes. Considering odd modes only, (23) in matrix form can be written as

$$\begin{bmatrix} 1 + M_{11} & \cdots & \cdot M_{1i} & \cdot\cdot \\ \vdots & & \vdots & \\ M_{i1}\cdot & \cdots & 1 + M_{ii} & \cdot\cdot \\ \cdot & \cdot & \cdot & \\ \cdot & & \cdot & \end{bmatrix} \cdot \begin{bmatrix} C^1 \\ \vdots \\ C^i \\ \cdot \\ \cdot \end{bmatrix} = 0, \qquad \text{odd modes only} \tag{25}$$

where M and C are matrices defined by

$$M_{ij} = \begin{bmatrix} \alpha_{ij} g_{11}^j & \alpha_{ij} g_{12}^j \\ \alpha_{ij} g_{21}^j 2 & \alpha_{ij} g_{22}^j \end{bmatrix} \qquad \begin{matrix} i = 1, 3, 5, \cdots \\ j = 1, 3, 5, \cdots \end{matrix} \tag{26}$$

and

$$C^i = \begin{bmatrix} c_1^i \\ c_2^i \end{bmatrix}. \tag{27}$$

An equation similar to (25) can also be written for the even modes.

For nontrivial unique solutions to c^n's, the infinite determinant of the coefficient matrix in (25) must be zero. The dispersion relation between ω and K is therefore obtained from the vanishing of this infinite determinant.

IV. Computer Results

For approximate numerical determination of the dispersion relation for the lowest order mode ($m = 1$), (25) is truncated to a finite order N and the determinant of the $N \times N$ matrix denoted by $D_N(\omega, K)$ is set to zero.

A computer program was developed to find the first root of

$$D_N(\omega, K) = 0 \tag{28}$$

TABLE I
COMPARISON OF RESULTS

Frequency f (GHz)	Exact Root K_o (cm^{-1})	N = 8 Approximate Root K_o' (cm^{-1})	Relative Error $[(K_o' - K_o)/K_o] \times 100$ (Percent)
7.5	- 1.145	- 1.147	0.14
7.9	- 2.050	- 2.053	0.15
8.9	- 5.379	- 5.382	0.05
9.5	- 9.748	- 9.760	0.12
9.9	- 22.843	- 23.011	0.73

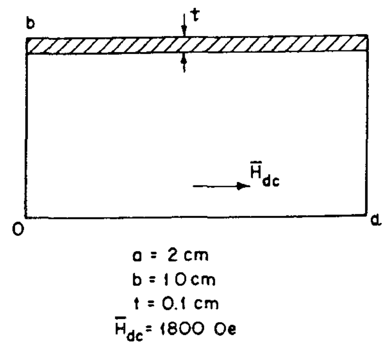

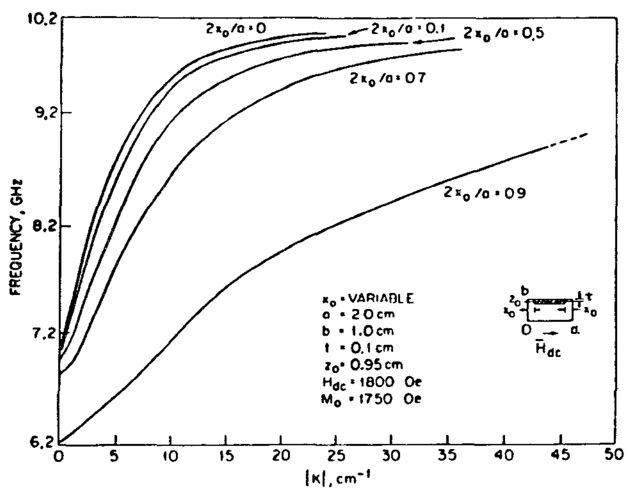

Fig. 3. Effect of increasing the air gap (x_o) on the dispersion curve.

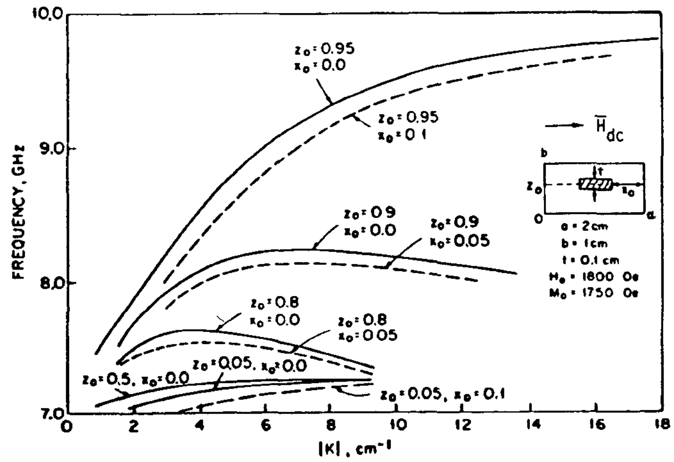

Fig. 4. Combined effect of position and width of the slab on the dispersion curves.

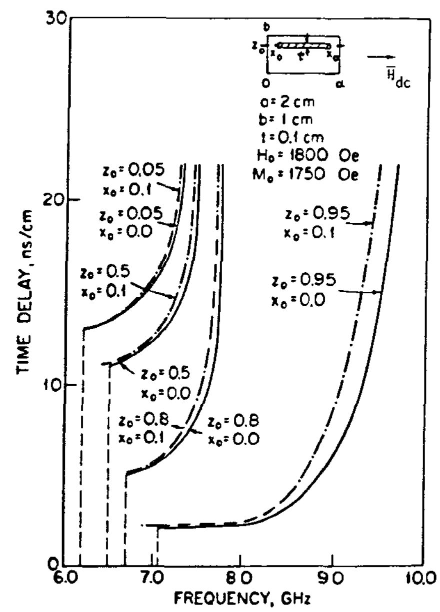

Fig. 5. Effect of slab width and position on time delay/unit length.

for a given ω. For meaningful results, computation of the first root was carried out for a sequence of increasing values of N until a convergent first root was obtained. In general, the cutoff number (N) increases with the gap size (x_0). A typical dependence of N with x_0 is shown in Fig. 2. The accuracy of our computer algorithm is also tested for the limiting case of $x_0 = 0$, for which exact results are obtained by mode analysis [7]. The comparison of numerical results using two different techniques is illustrated for a typical case in Table I. It appears from this table that the numerical algorithm is quite effective.

Several propagation properties and effects have been studied for the first-order mode and are briefly described in the rest of this section. The effect of increasing the normalized air gap ($2x_0/a$) on the dispersion relation for the special case when the slab is placed against the top of the guide is shown in Fig. 3. It is noted that the dispersion curves shift downward to lower frequencies as the air gap increases.

The combined effect of the position and width of the YIG slab is shown in Fig. 4. In this figure, the dispersion relations for several positions (z_0) of the slab, each position with two values of x_0, are presented. This figure shows that as the slab position is lowered, the dispersion curves are compressed with smaller bandwidths.

The corresponding group time delay per unit length in nanoseconds per centimeter defined by the relation $\tau_d = (\partial\omega/\partial K)^{-1}$ is shown in Fig. 5. From this figure, it is seen that for fixed time delay the operating frequency can be adjusted effectively by varying the position z_0, while for a fixed frequency the time delay can be increased by increasing the gap length x_0.

Tunable properties are also investigated by varying the magnetic bias field. Fig. 6 shows the effect of magnetic bias field on the dispersion curves for a particular geometry, that is, when $x_0 = 0$. As can be seen, the dispersion curves move up or down the $\omega - K$ plane by varying $\overline{H}_{dc}$.

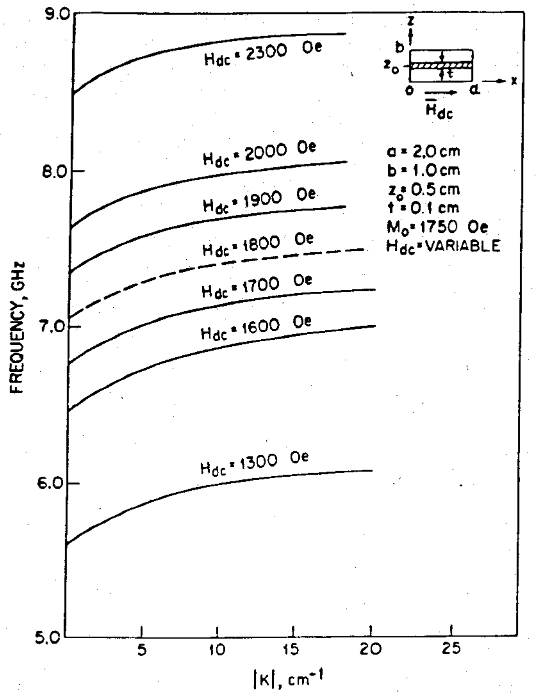

Fig. 6. Effect of magnetic bias field on the dispersion characteristics.

V. Conclusions

The propagation and time delay characteristics of magnetostatic waves in a waveguide partially filled with a YIG slab, with an equal air gap on each of its sides, were studied. Numerical results were presented for several chosen configurations over a frequency range of approximately 6.0–10.00 GHZ. The dependence of the dispersion relation and time delay per unit length on the position and width of the YIG slab were presented.

It is concluded that as the slab width decreases, the delay time increases and dispersion curves bandwidth shifts downward, while as the slab position is lowered the delay time increases and the dispersion curves are compressed with smaller bandwidths. This means that roughly speaking, the position of the slab controls the bandwidth and its width controls the center frequency of the device.

From Figs. 4 and 5, it is seen that in order to obtain high values of group time delay per unit length, the YIG slab must be narrow and placed at the bottom of the guide. On the other hand, to maximize the device bandwidth, a narrow YIG slab positioned at the top inside surface of the waveguide is preferred. It is also noticed that there exists a tradeoff between the time delay per unit length and the device bandwidth and maximization of one property leads to a poor value in the other. Thus, some design compromises should be made.

Finally, the tunable properties of the general structure by means of the magnetic bias field adds a new dimension of flexibility for its operation in any desired frequency range.

References

[1] R. W. Damon and J. R. Eshbach, "Magnetostatic modes of ferromagnetic slab," *J. Chem. Solids*, vol. 19, pp. 308–320, 1961.

[2] M-C. Tsai, H-J. Wu, J. M. Owens, and C. V. Smith, Jr., "Magnetostatic propagation for uniform normally-magnetized multilayer planar structure," in *AIP Conf. Proc.*, 1976, pp. 280–282.

[3] B. A. Auld and K. B. Mehta, "Magnetostatic waves in a transversely magnetized rectangular bar," *J. Appl. Phys.*, vol. 38, pp. 4081–4082, 1967.

[4] J. H. Collins, J. M. Owens, and C. V. Smith, Jr., "Magnetostatic wave signal processing," in *Ultrasonics Symp. Proc.*, 1977, pp. 541–552.

[5] J. D. Adam, J. H. Collins, and J. M. Owens, "Microwave device applications of epitaxial magnetic garnets," *Radio Electron. Eng.*, vol. 45, pp. 738–748, Dec. 1975.

[6] M. R. Daniel, J. D. Adam, and T. W. O'Keeffe, "Linearly dispersive delay lines at microwave frequencies using magnetostatic waves," in *Ultrasonic Symp. Proc.*, 1979, pp. 806–809.

[7] M. Radmanesh, C. M. Chu, and G. I. Haddad, "Magnetostatic-wave propagation in a yttrium iron garnet (YIG)-loaded waveguide," *Microwave J.*, vol. 29, no. 7, 1986.

[8] B. Lax and K. J. Button, *Microwave Ferrites and Ferrimagnetics*. New York: McGraw-Hill, 1962, ch. 4, pp. 145–151.

[9] B. Lax and K. J. Button, *Microwave Ferrites and Ferrimagnetics*. New York: McGraw-Hill, 1962, ch. 4, pp. 157–164.

Massoude Radmanesh received the B.S. degree in electrical engineering in 1978 from Pahlavi University, Shiraz, Iran. He earned the M.S.E.E. and Ph.D. degrees in electrical engineering and microwave electronics at the University of Michigan, Ann Arbor, MI, in 1980 and 1984, respectively.

During his studies at the University of Michigan, he was working on microwave solid-state devices (in particular, MSW devices) and FET modeling with Prof. G. I. Haddad. Since 1984, he has been a faculty member at the Electrical and Computer Engineering Department at GMI Engineering & Management Institute, Flint, MI. He has written several papers on magnetostatic-wave propagation in a YIG-loaded waveguide that are currently in the process of being published. His main area of interests are microwave solid-state devices, microwave integrated circuits, and wave propagation in anisotropic media. His current research is on MSW devices.

Chiao-Min Chu received the Ph.D. degree in electrical engineering from the University of Michigan, Ann Arbor, in 1952.

Since then he has held several appointments on the research staff at the University of Michigan. He joined the electrical engineering faculty of the University of Michigan as an Assistant Professor in 1956 and was promoted to Full Professor in 1963. He conducts a research in electrical transmission, wave propagation, and scattering of waves by conducting and dielectric particles, including scattering from terrain and the sea. He is currently conducting research in the area of wave propagation through anisotropic and random media, and the statistical analysis of signals scattered from random surfaces.

George I. Haddad (S–57, M'61–SM'66–F'72) was born in Aindara, Lebanon, on April 7, 1935. He received the B.S.E., M.S.E., and Ph.D. degrees in electrical engineering in 1956, 1958, and 1963, respectively, from The University of Michigan, Ann Arbor.

From 1957 to 1958, he was associated with the Engineering Research Institute of the University of Michigan, where he was engaged in research on electromagnetic accelerators. In 1958, he joined the Electron Physics Laboratory, where he was engaged in research on masers, parametric amplifiers, detectors, electron-beam devices. He is presently associated with the Solid-State Electronics Laboratory and doing research in microwave and millimeter-wave solid-state devices and monolithic integrated circuits. He served as Director of the Electron Physics Laboratory from 1968–1975. From 1960–1969, he served successively as Instructor, Assistant Professor, and Associate Professor in the Electrical Engineering Department. He is presently a Professor and Chairman of the Department of Electrical Engineering and Computer Science.

Dr. Haddad received the 1970 Curtis W. McGraw Research Award of the American Society for Engineering Education for outstanding achievements by an engineering teacher and the College of Engineering Excellence in Research Award in 1985. He is a member of Eta Kappa Nu, Sigma Xi, Phi Kappa Phi, Tau Beta Pi, and the American Society for Engineering Education.